

Synthesis and Properties of the Indenyl Ruthenium(II) Complex

[Ru{(E)- η^1 -C(C \equiv CPh)=CHPh)}(η^5 -C $_9$ H $_7$)(κ^2 -P-dppm)] (dppm = bis(diphenylphosphino)methane). An Organometallic Intermediate in the Catalytic Dimerization of Phenylacetylene

Mauro Bassetti* and Silvia Marini

Istituto CNR di Chimica dei Composti Organo Metallici, Sezione di Roma, c/o Dipartimento di Chimica, Università La Sapienza, 00185 Roma, Italy

Josefina Díaz, M. Pilar Gamasa, José Gimeno,* and Yolanda Rodríguez-Álvarez

Instituto de Química Organometálica Enrique Moles (Unidad Asociada al CSIC), Departamento de Química Orgánica e Inorgánica, Facultad de Química, Universidad de Oviedo, 33071 Oviedo, Spain

Santiago García-Granda

Departamento de Química Física y Analítica, Facultad de Química, Universidad de Oviedo, 33071 Oviedo, Spain

Received June 19, 2002

The reaction of the hydride complex [RuH(η^5 -C $_9$ H $_7$)(κ^2 -P-dppm)] (**1**) with an excess of 1,4-diphenyl-1,3-butadiene, PhC \equiv C–C \equiv CPh, yields complex [Ru{(E)- η^1 -C(C \equiv CPh)=CHPh)}(η^5 -C $_9$ H $_7$)(κ^2 -P-dppm)] (**3**), formed by regio- and stereoselective insertion of the alkyne into the Ru–H bond, in toluene or benzene-*d*₆. The reaction, about 4 times slower than with the terminal alkyne phenylacetylene, proceeds via an associative mechanism, characterized by the following activation parameters: $\Delta H^\ddagger = 11$ kcal mol⁻¹; $\Delta S^\ddagger = -44$ cal mol⁻¹ K⁻¹. The σ -enynyl complex **3** is protonated with an equimolar amount of HBF $_4$ ·Et $_2$ O to give the cationic alkynylalkylidene complex [Ru{=C(C \equiv CPh)CH $_2$ Ph)}(η^5 -C $_9$ H $_7$)(κ^2 -P-dppm)][BF $_4$] (**4**), which in turn is deprotonated by ^tBuOK to regenerate quantitatively complex **3**. Both complexes **3** and **4** have been characterized by X-ray structural analysis. Complex **3** catalyzes the dimerization of PhC \equiv CH to give (*E*)- and (*Z*)-1,4-diphenyl-1-buten-3-yne under milder conditions than analogous indenyl complexes [RuX(η^5 -C $_9$ H $_7$)(dppm)] (X = H, C \equiv CPh, (*E*)-CH=CHPh), while complex **4** is inactive. The σ -metathesis reaction between complex **3** and PhC \equiv CH is not the rate-determining step in the catalytic cycle.

Introduction

Various ruthenium complexes have been shown to be active catalysts for the dimerization of terminal alkynes to form disubstituted enynes (eq 1).¹



This reaction, of potential synthetic utility, involves C–H activation and satisfies the criteria of “atom economy”, where one substrate is converted into a

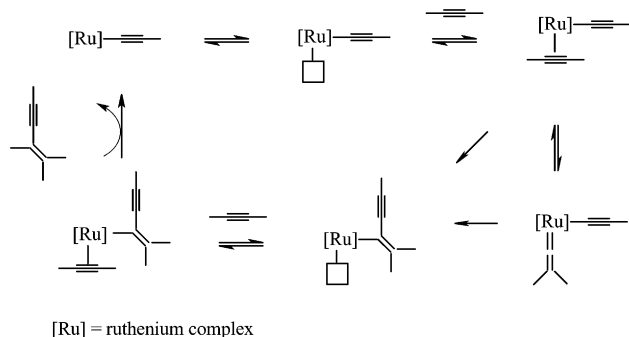
dissymmetric species without waste products.² Of main concern is still the regioselectivity due to competitive head-to-tail 1,3 or head-to-head 1,4 disubstitution, and to competitive formation of the two geometric isomers or of oligomers versus dimers. Significant progress regarding the catalytic efficiency has been obtained upon the use of ruthenium complexes bearing N-heterocyclic carbene ligands, which allow the dimerization reaction to proceed very rapidly at room temperature, rather than in refluxing solvents.³ Although the process has not been developed as a useful synthetic procedure, we have recently shown the possibility of obtaining and isolating from phenylacetylene both the *E* and *Z* isomers of 1,4-diphenyl-1-buten-3-yne, as an alternative to the Heck reaction or to more elaborate reaction sequences.⁴

(1) (a) Qu, J.-P.; Masui, D.; Ishii, Y.; Hidai, M. *Chem. Lett.* **1998**, 10, 1003. (b) Bruce, M. I.; Hinchliffe, J. R.; Humphrey, P. A.; Surynt, R. J.; Skelton, B. W.; White, A. H. *J. Organomet. Chem.* **1998**, 552, 109. (c) Yi, C. S.; Liu, N.; Rheingold, A. L.; Liable-Sands, L. M. *Organometallics* **1997**, 16, 3910. (d) Slugovc, C.; Mereiter, K.; Zöbets, E.; Schmid, R.; Kirchner, K. *Organometallics* **1996**, 15, 5275. (e) Wakatsuki, Y.; Koga, N.; Yamazaki, H.; Morokuma, K. *J. Am. Chem. Soc.* **1994**, 116, 8105. (f) Bianchini, C.; Peruzzini, M.; Zanobini, F.; Frediani, P.; Albinati, A. *J. Am. Chem. Soc.* **1991**, 113, 5453. (h) Echavarren, A. M.; López, J.; Santos, A.; Montoya, J. *J. Organomet. Chem.* **1991**, 414, 393. (g) Dahlenburg, L.; Frosin, K.-M.; Kerstan, S.; Werner, D. *J. Organomet. Chem.* **1991**, 407, 115.

(2) Trost, B. M. *Chem. Ber.* **1996**, 129, 1313.

(3) Baratta, W.; Herrmann, W. A.; Rigo, P.; Schwarz, J. *J. Organomet. Chem.* **2000**, 593–594, 489.

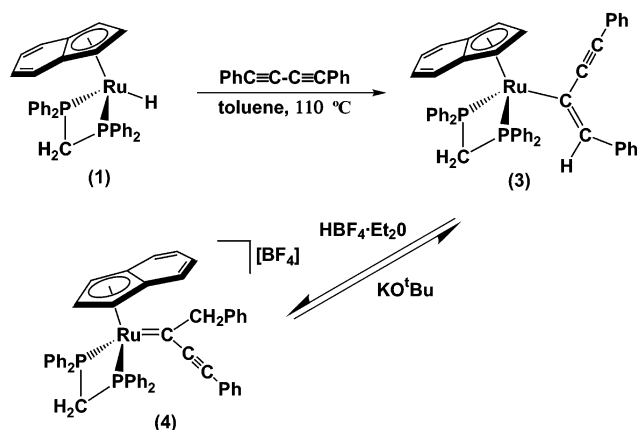
Scheme 1



Various authors have proposed a mechanistic scheme of the catalytic process, which can therefore be rationalized according to Scheme 1.¹ The key steps are generation of a free coordination site in a Ru-acetylide species, coordination of the alkyne, rearrangement of the π -complexed molecule to a vinylidene species,⁵ intramolecular acetylide migration to the α -vinylidene carbon to give a labile η^3 - or η^1 -butenyne complex, and σ -bond metathesis with an incoming alkyne molecule to form the organic enyne and the catalytic species. An alternative and short-cut step is the direct alkyne insertion into the Ru-acetylide bond, although the intermediacy of vinylidene species is highly favored. Since an acetylide complex can form by insertion of the alkyne into the Ru-H bond of dihydride species and subsequent transformations, ruthenium hydride complexes are also precatalysts of the dimerization process.⁶ The mechanistic features of the sequential formation of a diacetylide compound from the *cis*-dihydride complex [RuH₂(PP₃)] (PP₃ = P(CH₂CH₂PPh₂)₃) and the role of 1-alkyne as hydrogen donor to the acetylide fragment have been described in the dimerization of phenylacetylene.⁶

The formulation of the catalytic cycle as shown in Scheme 1 is based essentially on the logic assembly of known stoichiometric reactions, rather than on experimental evidence of intermediates or sequence of steps. As a consequence, the current understanding of the process does not allow the design of an efficient and selective precatalyst, nor to know which are the rate- and stereo-determining steps. For instance, the reasonable assumption that the catalytic precursor bearing a Ru-acetylide moiety, i.e., one partner of the coupling step,^{1c,6} may more efficiently enter the catalytic cycle has not met with the experimental results, except for the case of the bis-acetylide complex [Ru(C≡CPh)₂(PP₃)].⁶ In fact, comparable results have been obtained using an alkynyl complex containing a hemilabile ligand [Ru(C≡CPh)Tp(κ^2 (P,O)-Ph₂PCH₂CH₂OMe)] (Tp = hydridotrispyrazolylborate) or the complexes [RuHTp(PPH₃)₂], [Ru(=C=CHPh)TpCl], and [RuH₃(η^5 -C₅Me₅)(PR₃)].⁷ We have also observed that the nature of the anionic η^1 -ligand does not affect significantly the catalytic activity of the indenyl complexes [RuX(η^5 -C₉H₇)(dppm)] (X = H, C≡CPh, (*E*)-CH=CHPh).⁴

Scheme 2



Since Ru- σ -enynyl species have been proposed as intermediates and many complexes of this type have been isolated,^{1c,d,7} we have focused our attention on this species, as a potential source of information about the catalytic cycle. We report now (a) the synthesis and structural characterization of [Ru{(*E*)- η^1 -C(C≡CPh)=CHPh]}(η^5 -C₉H₇)(dppm) (**3**), formed by insertion of 1,4-diphenylbutadiyne (**2**) into the Ru-H bond of [RuH(η^5 -C₉H₇)(dppm)] (**1**), (b) the kinetics of this reaction, and (c) the catalytic properties of **3** in the dimerization of phenylacetylene. We have previously described a kinetic study of the insertion of phenylacetylene into the Ru-H bond of [RuH(η^5 -C₉H₇)(dppm)] to give the corresponding vinyl derivative.⁸

Results and Discussion

Synthesis of the Enynyl Complex [Ru{(E)- η^1 -C(C≡CPh)=CHPh]}(η^5 -C₉H₇)(κ^2 -P-dppm) (3**).** The reaction of the hydride complex [RuH(η^5 -C₉H₇)(κ^2 -P-dppm)] (**1**) with a 10-fold excess of diphenylbutadiyne (**2**) in refluxing toluene leads to the formation of the enynyl complex **3** (58%). The low yield of recovered complex is due to the separation procedure from the diene, which involves washings with pentane of the crude product. On the other hand, the reaction of **1** with an equimolar amount of **2** gave in addition to complex **3** consistent formation of an uncharacterized species (³¹P{¹H} NMR signal at δ 22.9 ppm). This byproduct is still formed when using a 5-fold amount of diene, but it is not detected at larger excesses. Complex **3** is easily protonated with an equimolar amount of HBF₄·Et₂O in diethyl ether to give the alkynylalkylidene complex **4** (see below) in nearly quantitative yield. The sequence of protonation of **3** in the crude reaction mixture to give **4** followed by deprotonation of **4** to give back **3** has been employed to improve the yield of **3** (81%) (see Scheme 2 and Experimental Section).

Complex **3** has been isolated as an air-stable yellow-orange solid and characterized by mass spectrum (FAB) and IR and NMR spectroscopy. The ³¹P{¹H} NMR spectrum shows a singlet signal at δ 19.68, indicating the chemical equivalence of both phosphorus atoms. The IR and ¹H and ¹³C{¹H} NMR spectra show the expected resonances arising from the presence of the indenyl,

(4) Bassetti, M.; Marini, S.; Tortorella, F.; Cadierno, V.; Díez, J.; Gamasa, M. P.; Gimeno, J. *J. Organomet. Chem.* **2000**, 593–594, 292.

(5) Cadierno, V.; Gamasa, M. P.; Gimeno, J.; González-Bernardo, C.; Pérez-Carreño, E.; García-Granda, S. *Organometallics* **2001**, 20, 5177.

(6) Bianchini, C.; Frediani, P.; Masi, D.; Peruzzini, M.; Zanobini, F. *Organometallics* **1994**, 13, 4616.

(7) Pavlik, S.; Gemel, C.; Slugovc, C.; Mereiter, K.; Schmid, R.; Kirchner, K. *J. Organomet. Chem.* **2001**, 617–618, 301.

(8) Bassetti, M.; Casellato, P.; Gamasa, M. P.; Gimeno, J.; Gonzales-Bernardo, C.; Martin-Vaca, B. *Organometallics* **1997**, 16, 5470.

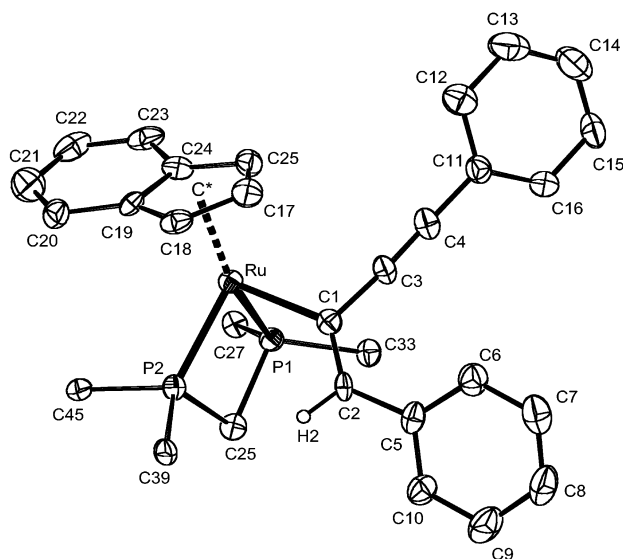


Figure 1. ORTEP view of complex $[\text{Ru}\{\eta^5\text{-}C_9\text{H}_7\}(\kappa^2\text{-}P\text{-dppm})\{\eta^1\text{-}C(\text{C}\equiv\text{CPh})=\text{CHPh}\}]$ (**3**). Thermal ellipsoids are shown at the 30% level. For clarity, the H atoms, except that of the enyne moiety, and the phenyl rings of bis(diphenylphosphino)methane are omitted.

phosphine, and enynyl groups. Significantly, the presence of the enynyl moiety was identified on the basis of (i) a $\nu(\text{C}\equiv\text{C})$ absorption in the IR spectrum (KBr) at 2154 cm^{-1} , (ii) a singlet signal in the ^1H NMR spectrum at δ 5.56 (C=CH), (iii) two singlet resonances at 99.91 and 102.32 ppm for $\equiv\text{CPh}$ and $\text{C}\equiv\text{CPh}$, respectively, and two triplets at δ 134.35 ($^2J_{\text{CP}} = 13.7\text{ Hz}$) and 145.01 ($^3J_{\text{CP}} = 5.8\text{ Hz}$) ppm for the carbon atoms of the alkenyl group in the $^{13}\text{C}\{^1\text{H}\}$ NMR spectrum. To assign the regio- and stereochemistry of the alkenyl group, an X-ray crystal structure determination of complex **3** has been carried out. An ORTEP type view is shown in Figure 1, and selected bond distances and angles are listed in Table 1.

The molecular structure shows the typical pseudooctahedral three-legged piano-stool geometry around the ruthenium atom, which is linked to the η^5 -indenyl group, to the two phosphorus atoms of the chelate diphosphine, and to the C(1) of the enynyl ligand, resulting from a regio- and stereoselective (*cis*) insertion of diphenylbutadiyne into the Ru–H bond.

The bite angle of the chelate *dppm* ligand P(1)–Ru–P(2) ($71.31(8)^\circ$) shows a value similar to the one in complex $[\text{RuH}(\eta^5\text{-}C_9\text{H}_7)(\kappa^2\text{-}P\text{-dppm})]$ ($71.28(2)^\circ$)⁹ and in the analogous chelate *S-peap* of the alkenyl complex $[\text{Ru}\{\eta^5\text{-}C_9\text{H}_7\}(\kappa^2\text{-}P\text{-}S\text{-peap})\{\eta^1\text{-}C(\text{CO}_2\text{Me})=\text{CH}(\text{CO}_2\text{Me})\}]$ ($70.53(9)^\circ$) (*S-peap* = (–)-*N,N*-bis(diphenylphosphine)-*S*- α -phenylethylamine).¹⁰ The bond length distance Ru–C(1), $2.094(7)^\circ$, is analogous to those reported in other alkenyl ruthenium complexes.¹⁰ The C(1)–C(2) ($1.349(10)^\circ$) and C(3)–C(4) ($1.182(10)^\circ$) distances are typical of a double and triple carbon–carbon bond, respectively, such as those found in other σ -butenylnyl ligands.¹¹ The rest of the main structural parameters,

Table 1. Selected Bond Distances and Slip Parameter Δ^a (Å) and Bond Angles and Dihedral Angles HA,^b FA,^c and CA^d (deg) for Complex **3**

Distances			
Ru–C*	1.976(10)	Ru–C(24)	2.404(10)
Ru–C(1)	2.094(7)	Ru–C(25)	2.291(10)
Ru–P(1)	2.302(3)	C(1)–C(2)	1.349(10)
Ru–P(2)	2.265(3)	C(1)–C(3)	1.422(11)
Ru–C(17)	2.241(9)	C(3)–C(4)	1.182(10)
Ru–C(18)	2.246(10)	C(4)–C(11)	1.438(13)
Ru–C(19)	2.395(9)	C(2)–C(5)	1.482(10)
Δ	0.130(10)		
Angles			
P(1)–Ru–P(2)	71.31(8)	Ru–C(1)–C(3)	108.6(6)
P(1)–Ru–C(1)	81.3(2)	Ru–C(1)–C(2)	129.3(6)
P(2)–Ru–C(1)	94.6(2)	C(3)–C(1)–C(2)	122.0(7)
C*–Ru–P(1)	143.7(3)	C(1)–C(3)–C(4)	174.5(9)
C*–Ru–P(2)	131.4(3)	C(3)–C(4)–C(11)	174.6(10)
C*–Ru–C(1)	117.9(4)	C(1)–C(2)–C(5)	130.8(7)
HA	4.4(8)	CA	5.9(5)
FA	8.7(7)		

^a $\Delta = d[\text{Ru}–\text{C}(19), \text{C}(24)] - d[\text{Ru}–\text{C}(18), \text{C}(25)]$. ^b HA (hinge angle) = angle between normals to least-squares planes defined by [C(25), C(17), C(18)] and [C(18), C(19), C(24), C(25)]. ^c FA (fold angle) = angle between normals to least-squares planes defined by [C(25), C(17), C(18)] and [C(19), C(20), C(21), C(22), C(23), C(24)]. ^d CA (conformational angle) = angle between normals to least-squares planes defined by [C*, C*, Ru] and [C*, Ru, C(1)]. C* = centroid of C(17), C(18), C(19), C(24), C(25). C** = centroid of C(19), C(20), C(21), C(22), C(23), C(24).

i.e., Ru–P(1) = $2.302(3)\text{ \AA}$, Ru–P(2) = $2.265(3)\text{ \AA}$, Ru–C* = $1.976(10)\text{ \AA}$ (C* = centroid of the five-membered indenyl ring), hinge angle (HA) = $4.4(8)^\circ$, fold angle (FA) = $8.7(7)^\circ$, slippage parameter (Δ) = $0.130(10)\text{ \AA}$, can be compared with those found in analogous indenyl-phosphinoruthenium(II) complexes reported by us and do not merit further comment.¹² The most remarkable structural feature is the *E* configuration of the alkenyl group showing the alkenyl substituent attached to the C_α atom. It is also worth noting the nearly *trans* orientation of the alkenyl group with respect to the benzo ring of the indenyl ligand (CA = $5.9(5)\text{ \AA}$) and the orientation of the alkenyl substituent of the alkenyl group, defined by the dihedral angle ($52.1(5)^\circ$) formed by the planes Ru–C(1)–C(3) and Ru–C(1)–C*.

The preparation of complex **3** via reaction of the hydride complex **1** with diphenylbutadiyne to form σ -butenylnyl complexes is not common. These species are obtained by reaction of alkenyl ruthenium derivatives with a terminal alkyne,^{14,7} by reaction of a vinylidene complex with $\text{LiC}\equiv\text{C}^t\text{Bu}$,¹¹ by protonation of a bis(σ -alkynyl) ruthenium complex and subsequent coupling,⁶ or by carbon–carbon coupling in alkenyl-vinylidene complexes.¹³ When $[\text{Ru}(\text{C}\equiv\text{CPh})(\eta^5\text{-}C_9\text{H}_7)(\text{dppm})]$ is allowed to react with $\text{PhC}\equiv\text{CH}$ in toluene, (*E*)- and (*Z*)-1,4-diphenyl-1-buten-3-yne form at elevated temperatures as the only organic products, while the alkenyl complex is the only organometallic species observed by ^{31}P and ^1H NMR, maintaining constant concentration throughout the reaction. This implies rate-limiting reaction of the alkenyl with the alkyne followed by fast σ -metathesis with a second alkyne molecule to form the organic products, the presumed σ -enynyl complex not

(9) Hung, M. Y.; Ng, S. M.; Zhou, Z.; Lau, C. P.; Jia, G. *Organometallics* **2000**, *19*, 3692.

(10) Bieger, K.; Díez, J.; Gamasa, M. P.; Gimeno, J.; Pavlista, M.; Rodríguez-Alvarez, Y.; García-Granda, S.; Santiago-García, R. *Eur. J. Inorg. Chem.* **2002**, *7*, 1647.

(11) Wakatsuki, Y.; Yamazaki, H.; Kumegawa, N.; Satoh, T.; Satoh, J. Y. *J. Am. Chem. Soc.* **1991**, *113*, 9604.

(12) Cadierno, V.; Díez, J.; Gamasa, M. P.; Gimeno, J.; Lastra, E. *Coord. Chem. Rev.* **1999**, *193–195*, 147.

(13) Albertin, G.; Antoniutti, S.; Bordignon, E.; Cazzaro, F.; Ianelli, S.; Pelizzi, G. *Organometallics* **1995**, *14*, 4114.

being detectable (Scheme 1). In the case of $[\text{Ru}(\text{PP}_3)(\text{C}\equiv\text{CSiMe}_3)][\text{BF}_4]$ reacting with $\text{Me}_3\text{SiC}\equiv\text{CH}$,^{1f} or of $[\text{Ru}(\text{C}\equiv\text{CPh})\text{Tp}(\kappa^2(\text{P},\text{O})\text{-Ph}_2\text{PCH}_2\text{CH}_2\text{OMe})]$ reacting with $\text{PhC}\equiv\text{CH}$,⁷ η^3 -butenyne complexes are stable and isolable materials. It is possible that such enynyl complexes via this route are stabilized by the η^3 -coordination mode, which is allowed by the four-donor system (P_4) in one case^{1f} and by the hemilabile character of the phosphinoether ligand in the other.⁷

The insertion of a 1,4-butadiyne into Ru-H has been used to form $[\text{Ru}\{\text{(E)-}\eta^1\text{-C}(\text{C}\equiv\text{C}^t\text{Bu})=\text{CH}^t\text{Bu}\}\text{Cl}(\text{CO})(\text{PPh}_3)_2]$ from $(^t\text{BuC}\equiv\text{C})_2$ and $[\text{RuClH}(\text{CO})(\text{PPh}_3)_3]$.¹⁴ This η^1 -enynyl complex decomposed thermally to release (*Z*)-1,4-di-*tert*-butylbutatriene.

Synthesis of the Alkynylalkylidene Complex $[\text{Ru}\{\text{C}(\text{C}\equiv\text{CPh})\text{CH}_2\text{Ph}\}(\eta^5\text{-C}_9\text{H}_7)(\kappa^2\text{-P-dppm})][\text{BF}_4]$ (4**).** Complex **3** reacts with $\text{HBF}_4\cdot\text{Et}_2\text{O}$ at -40°C , in diethyl ether, producing instantaneously the precipitation of complex **4**, which is isolated from the reaction mixture as an air-stable red solid (94%). This complex is easily deprotonated with an equimolar amount of $\text{KO}^t\text{-Bu}$ in THF to give the enynyl complex **3** in quantitative yield.

Complex **4** has been characterized by mass spectrum (FAB), conductance measurement, and IR and NMR spectroscopy, which support the proposed formulation. Conductivity data, in acetone solution, are in the range expected for a 1:1 electrolyte, and the IR spectrum exhibits the typical $\nu(\text{B-F})$ strong absorption at 1062 cm^{-1} . ^1H and $^{13}\text{C}\{^1\text{H}\}$ NMR spectra reveal the presence of the alkenylalkylidene group; the most relevant data arise from the $^{13}\text{C}\{^1\text{H}\}$ NMR spectrum, which shows a typical low-field resonance at δ 293.78 (t, $^2J_{\text{CP}} = 6.4\text{ Hz}$) for the C_α atom and the higher field resonances assigned to the remaining carbon atoms of the hydrocarbon chain at δ 63.75 (s) (CH_2Ph), 108.78 (t, $^3J_{\text{CP}} = 3.1\text{ Hz}$), and 122.6 (s) ($\text{C}\equiv\text{CPh}$). These assignments can be compared to those recently reported for the rhenium complex $[\text{Re}\{\text{C}(\text{C}\equiv\text{CC}_6\text{H}_4\text{-}i\text{-P-CH}_3)(\text{C}_6\text{H}_4\text{-}i\text{-P-CF}_3)\}(\eta^5\text{-C}_9\text{H}_7)(\text{CO})_2]$.¹⁵ The formation of **4** is in accordance with the expected reactivity of alkenyl complexes, which are prone to undergo electrophilic additions at the C_β atom.¹⁶ Alkynylalkylidene complexes are scarcely found in the literature, and to the best of our knowledge, only the complex $[\text{Ru}\{\text{C}(\text{C}\equiv\text{CPh})\text{CH}=\text{CPh}_2\}(\eta^5\text{-C}_5\text{H}_5)(\text{CO})(\text{P}^i\text{-Pr}_3)][\text{BF}_4]$, with ruthenium, has been reported.¹⁷ The structure of complex **4** has been confirmed by an X-ray diffraction study. An ORTEP type view of the cation complex is shown in Figure 2, and selected bond distances and angles are collected in Table 2.

The pseudooctahedral geometry around the ruthenium atom is quite similar to that found for complex **3**, wherein the alkylidene group occupies the position of the former alkenyl moiety. Bonding distances, $\text{Ru-C}^* = 1.974(7)\text{ \AA}$, $\text{Ru-P}(1) = 2.265(2)\text{ \AA}$, $\text{Ru-P}(2) = 2.266(2)\text{ \AA}$, the chelating bite angle, $\text{P}(1)\text{-Ru-P}(2) = 72.64$

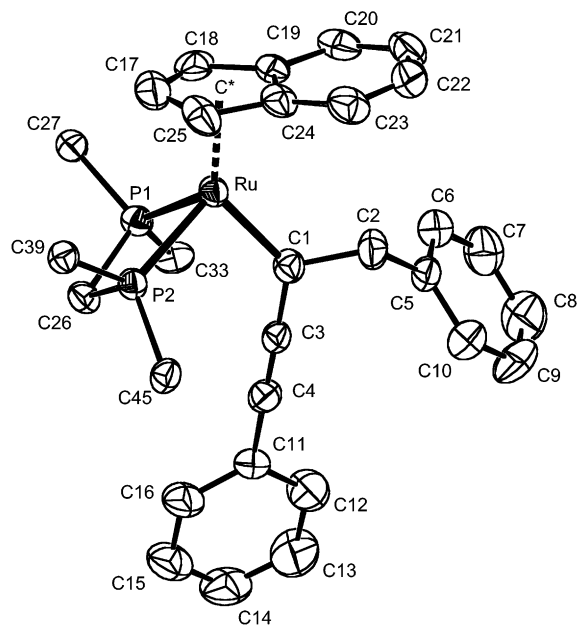


Figure 2. ORTEP view of complex $[\text{Ru}\{\text{C}(\text{C}\equiv\text{CPh})\text{CH}_2\text{Ph}\}(\eta^5\text{-C}_9\text{H}_7)(\kappa^2\text{-P-dppm})][\text{BF}_4]$ (**4**). Thermal ellipsoids are shown at the 30% level. For clarity, the H atoms and the phenyl rings of bis(diphenylphosphino)methane are omitted.

Table 2. Selected Bond Distances and Slip Parameter Δ^a (\AA) and Bond Angles and Dihedral Angles HA, b FA, c and CA d (deg) for Complex **4**

Distances			
Ru-C*	1.974(7)	Ru-C(24)	2.401(7)
Ru-C(1)	1.931(6)	Ru-C(25)	2.264(9)
Ru-P(1)	2.265(2)	C(1)-C(2)	1.522(8)
Ru-P(2)	2.266(2)	C(1)-C(3)	1.407(8)
Ru-C(17)	2.238(8)	C(3)-C(4)	1.199(8)
Ru-C(18)	2.247(7)	C(4)-C(11)	1.445(9)
Ru-C(19)	2.389(6)	C(2)-C(5)	1.497(10)
Δ	0.140(6)		
Angles			
P(1)-Ru-P(2)	72.64 (6)	Ru-C(1)-C(3)	127.7(4)
P(1)-Ru-C(1)	92.5(2)	Ru-C(1)-C(2)	119.2(4)
P(2)-Ru-C(1)	91.5(2)	C(2)-C(1)-C(3)	113.1(5)
C*-Ru-P(1)	123.2(2)	C(1)-C(3)-C(4)	177.0(7)
C*-Ru-P(2)	124.9(2)	C(3)-C(4)-C(11)	175.4(7)
C*-Ru-C(1)	133.5(3)	C(1)-C(2)-C(5)	115.4(5)
HA	5.4(6)	CA	5.5(4)
FA	10.2(5)		

^a $\Delta = d[\text{Ru-C}(19), \text{C}(24)] - d[\text{Ru-C}(18), \text{C}(25)]$. ^b HA (hinge angle) = angle between normals to least-squares planes defined by $[\text{C}(25), \text{C}(17), \text{C}(18)]$ and $[\text{C}(18), \text{C}(19), \text{C}(24), \text{C}(25)]$. ^c FA (fold angle) = angle between normals to least-squares planes defined by $[\text{C}(25), \text{C}(17), \text{C}(18)]$ and $[\text{C}(19), \text{C}(20), \text{C}(21), \text{C}(22), \text{C}(23), \text{C}(24)]$. ^d CA (conformational angle) = angle between normals to least-squares planes defined by $[\text{C}^*, \text{C}^*, \text{Ru}]$ and $[\text{C}^*, \text{Ru}, \text{C}(1)]$. C^* = centroid of $\text{C}(17), \text{C}(18), \text{C}(19), \text{C}(24), \text{C}(25)$. C^{**} = centroid of $\text{C}(19), \text{C}(20), \text{C}(21), \text{C}(22), \text{C}(23), \text{C}(24)$.

(6)°, and all the distortion parameters of the indenyl group (HA, FA, and Δ) are comparable to those shown for complex **3** (see Table 1).

Of special interest is the nearly *cis* orientation of the alkylidene chain relative to the benzo ring of the indenyl ligand ($\text{CA} = 5.5(4)\text{ \AA}$). A relevant feature is the orientation of the alkynyl substituent determined by the value of the dihedral angle defined by the planes $\text{Ru-C}(1)\text{-C}(3)$ and $\text{Ru-C}(1)\text{-C}^*$ ($176.5(5)^\circ$), which are nearly coplanar in **4**. This value contrasts with that shown in complex **3** ($52.1(5)^\circ$), and the difference probably arises

(14) Wakatsuki Y.; Yamazaki, H. *J. Organomet. Chem.* **1995**, *500*, 349.

(15) Casey, C. P.; Kraft, S.; Powell, D. R. *Organometallics* **2001**, *20*, 2651.

(16) (a) Gamasa, M. P.; Gimeno, J.; Martín-Vaca, B. M. *Organometallics* **1998**, *17*, 3707. (b) Harlow, K. J.; Hill, A. F.; Welton, T. *J. Chem. Soc., Dalton Trans.* **1999**, 1911. (c) Kostic, N. M.; Fenske, R. F. *Organometallics* **1982**, *1*, 974.

(17) Esteruelas, M. A.; Gómez, A. K.; López, A. M.; Modrego, J.; Oñate, E. *Organometallics* **1997**, *16*, 5826.

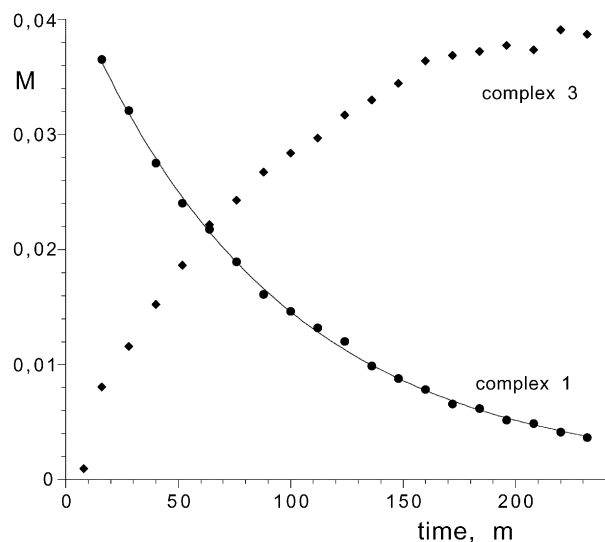


Figure 3. Plot of concentration values vs time for the reaction of complex $[\text{RuH}(\eta^5\text{-C}_9\text{H}_7)(\kappa^2\text{-P-dppm})]$ (\bullet , **1**) with $\text{PhC}\equiv\text{C}-\text{C}\equiv\text{CPh}$ (1.05 M) to give complex $[\text{Ru}\{\text{E}-\eta^1\text{-C}(\text{C}\equiv\text{CPh})=\text{CHPh}\}(\eta^5\text{-C}_9\text{H}_7)(\kappa^2\text{-P-dppm})]$ (\blacklozenge , **3**), in benzene- d_6 at 69 °C, by $^{31}\text{P}\{^1\text{H}\}$ NMR spectroscopy.

from the greater steric hindrance between the indenyl and the alkenyl group in **4**.

Kinetics of the Reaction of $[\text{RuH}(\eta^5\text{-C}_9\text{H}_7)(\text{dppm})]$ with $\text{PhC}\equiv\text{C}-\text{C}\equiv\text{CPh}$. The reaction of the hydride complex with 1,4-diphenylbutadiyne (**2**) in benzene- d_6 can be followed conveniently by $^{31}\text{P}\{^1\text{H}\}$ NMR spectroscopy, monitoring the disappearance of **1** (δ 20.3 ppm) as well as the formation of the σ -enynyl complex **3** (δ 19.7 ppm), while intermediate species are not detected. This is shown graphically in Figure 3.

The solid line represents the best exponential decay fitted to the data set of concentration values (c) vs time (t), according to the first-order rate equation (eq 2):

$$c_t = c_\infty + (c_0 - c_\infty) \exp -(k_{\text{obs}}t) \quad (2)$$

The experiment of Figure 3 yields a value of the observed rate constant, $k_{\text{obs}} = 1.1 \times 10^{-2} \text{ min}^{-1}$ at $[\mathbf{2}] = 1.05 \text{ M}$, corresponding to $\tau_{1/2}$ (half time) = 1 h ($T = 69$ °C). The reaction is first-order in the hydride complex. The reaction order on the diyne was investigated by varying the initial concentration of **2** in different experiments. Values of k_{obs} are reported in Table 4.

A plot of k_{obs} vs time is linear, which indicates first-order dependence on 1,4-diphenylbutadiyne as well; therefore that the reaction is overall second-order. The reaction of the deuteride complex $[\text{RuD}(\eta^5\text{-C}_9\text{H}_7)(\text{dppm})]$ proceeded at a rate similar to that of complex **1** (footnote c in Table 4). From the measurements carried out in the temperature range 43–69 °C, the following activation parameters were obtained: $\Delta H^\ddagger = 11 \pm 2 \text{ kcal mol}^{-1}$; $\Delta S^\ddagger = -44 \pm 5 \text{ cal mol}^{-1} \text{ K}^{-1}$. The data are consistent with the occurrence of an associative mechanism, as represented in Scheme 3 and described by eq 3,

$$k_{\text{obs}} = \frac{k_1 k_2 [(\text{PhC}\equiv\text{C})_2]}{k_{-1} + k_2} \quad (3)$$

in analogy with the results obtained for the reaction of complex **1** with phenylacetylene.⁸ This mechanistic

Table 3. Crystallographic Data for the Complexes **3 and **4****

	3	4
formula	$\text{C}_{50}\text{H}_{40}\text{P}_2\text{Ru}$	$\text{C}_{50}\text{H}_{41}\text{BF}_4\text{P}_2\text{Ru}$
fw	803.83	891.65
cryst syst	monoclinic	monoclinic
space group	$P2_1/c$	$P2_1/c$
a (Å)	13.255(5)	20.638(4)
b (Å)	17.082(10)	11.067(5)
c (Å)	17.651(6)	18.819(5)
α (deg)	90	90
β (deg)	96.98(3)	95.319(12)
γ (deg)	90	90
V (Å ³)	3967(3)	4280(2)
Z	4	4
calcd density (g cm ⁻³)	1.346	1.384
$F(000)$	1656	1824
radiation (λ , Å)	Mo K α (0.71073)	Mo K α (0.71073)
cryst size (mm)	0.20 × 0.13 × 0.07	0.33 × 0.20 × 0.20
temp (K)	293(2)	293(2)
monochromator	graphite cryst	graphite cryst
μ (mm ⁻¹)	0.510	0.493
diffraction geom	$\omega-2\theta$	$\omega-2\theta$
θ range for data collection (deg)	1.55–25.97	2.30–25.98
index ranges for data collection	$-16 \leq h \leq 16$	$-25 \leq h \leq 25$
	$-21 \leq k \leq 0$	$0 \leq k \leq 13$
	$-21 \leq l \leq 0$	$-23 \leq l \leq 0$
no. of reflns measd	8038	8679
no. of indep reflns	7772	8390
no. of variables	484	517
agreement between equiv reflns	0.0630	0.0348
final R factors ($I < 2\sigma(I)$)	R1 = 0.0483 wR2 = 0.0850	R1 = 0.0554 wR2 = 0.1390
final R factors (all data)	wR1 = 0.3175 wR2 = 0.1362	R1 = 0.1531 wR2 = 0.1741

Table 4. Observed Rate Constants, k_{obs} (s⁻¹), for the Reaction of $[\text{RuH}(\eta^5\text{-C}_9\text{H}_7)(\text{dppm})]$ (1**) with $\text{PhC}\equiv\text{C}-\text{C}\equiv\text{CPh}$ (**2**) in Benzene- d_6 ^a**

T (°C)	[1], M	[2], M	$-\text{d}[\mathbf{1}]/\text{d}t$ (s ⁻¹) ^b	k_1 (M ⁻¹ , s ⁻¹)
69	0.034	0.35	7.3×10^{-5}	
69	0.037	0.53 ^c	8.5×10^{-5}	
69	0.035	0.76	1.3×10^{-4}	
69	0.042	1.05	1.8×10^{-4}	
69				1.6×10^{-4} ^d
56	0.036	0.77	8.2×10^{-5}	1.06×10^{-4}
43.5	0.044	0.73	0.30×10^{-4}	0.41×10^{-4}

^a Method: $^{31}\text{P}\{^1\text{H}\}$ NMR spectroscopy (**1**, 20.3 ppm). ^b All values $\pm 10\%$. ^c $k_{\text{obs}} = 10 \times 10^{-5} \text{ s}^{-1}$ for the reaction of **2** (0.54 M) with $[\text{RuD}(\eta^5\text{-C}_9\text{H}_7)(\text{dppm})]$ (0.046 M). ^d Value obtained from the slope of k_{obs} vs $[\mathbf{2}]$.

scheme was proposed earlier for the insertion reaction of $^t\text{BuC}\equiv\text{CH}$ with the iridium hydride complex $[\text{IrH}(\text{Me})(\eta^5\text{-C}_9\text{H}_7)(\text{PMe}_3)]$.¹⁸ The intermediate of Scheme 3 may involve rate-determining π -coordination of the alkyne assisted by an η^5 - to η^3 -haptotropic shift of the indenyl ligand.¹⁹ The reactivity of the diyne toward **1** is about 4 times lower than that of the terminal alkyne ($k_1 = 0.41 \times 10^{-4} \text{ M}^{-1} \text{ s}^{-1}$ for $(\text{PhC}\equiv\text{C})_2$ at 43.5 °C in benzene- d_6 vs $k_1 = 1.8 \times 10^{-4} \text{ M}^{-1} \text{ s}^{-1}$ for $\text{PhC}\equiv\text{CH}$ at 40 °C in toluene- d_8), in a process that proceeds with identical stereochemical features and similar kinetic pattern. This may be due to greater steric hindrance of the diyne, as pointed out by the larger negative value

(18) Foo, T.; Bergman, R. G. *Organometallics* **1992**, *11*, 1811.

(19) (a) O'Connor, J. M.; Casey, C. P. *Chem. Rev.* **1987**, *87*, 307. (b) Calhorda, M. J.; Romao, C. C.; Veiros, L. F. *Chem. Eur. J.* **2002**, *8*, 868. (c) Veiros, L. F. *Organometallics* **2000**, *19*, 3127.

Scheme 3

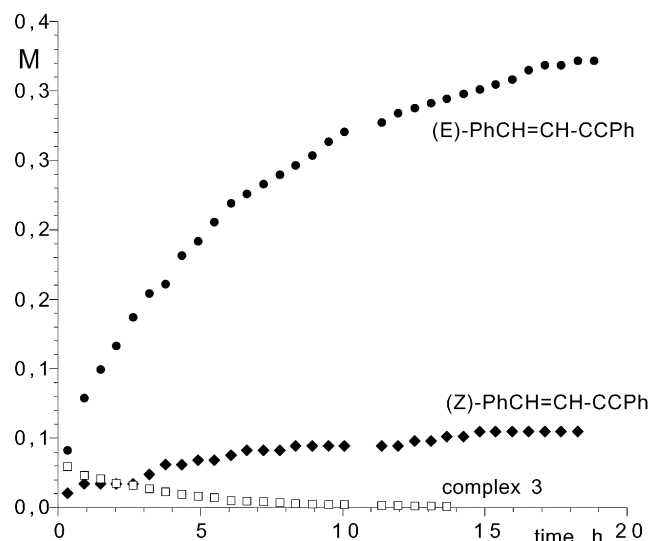
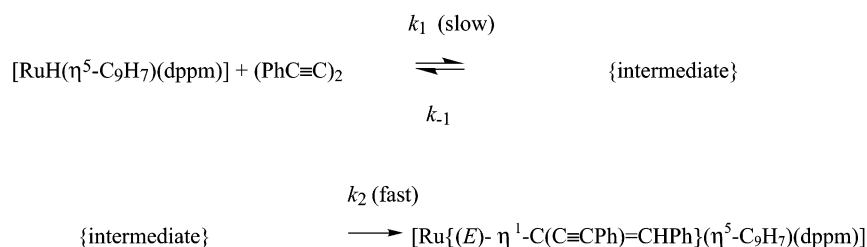


Figure 4. Reaction profile for the catalytic dimerization of phenylacetylene (4.2 M) in the presence of complex $[\text{Ru}\{(E)\text{-}\eta^1\text{-C}(\text{C}\equiv\text{CPh})\text{=CHPh}\}(\eta^5\text{-C}_9\text{H}_7)(\kappa^2\text{-P-dppm})]$ (0.059 M, 1.4%, **3**), showing the disappearance of **3** (\square) and the formation of (*E*, \bullet)- and (*Z*, \blacklozenge)-1,4-diphenyl-1-buten-3-yne, in benzene- d_6 at 77 °C.

of entropy of activation ($\text{PhC}\equiv\text{CH}$: $\Delta S^\ddagger = -21 \pm 4 \text{ cal mol}^{-1} \text{ K}^{-1}$).

Catalytic Properties of $[\text{Ru}\{(E)\text{-}\eta^1\text{-C}(\text{C}\equiv\text{CPh})\text{=CHPh}\}(\eta^5\text{-C}_9\text{H}_7)(\text{dppm})]$. Complex **3** was found to catalyze the dimerization of phenylacetylene. The reaction of $\text{PhC}\equiv\text{CH}$ (4.2 M) in the presence of **3** (0.059 M, 1.4%), in benzene- d_6 , was monitored by ^1H NMR, at constant temperature (77 °C). Figure 4 shows the disappearance of complex **3** and the formation of the products of homocoupling, (*E*)- and (*Z*)-1,4-diphenylbut-1-en-3-yne. After 15 h of reaction, more than 10 mol of enyne per mole of ruthenium complex has formed, with 44% conversion of the alkyne. The cationic complex **4** yields traces of the enyne products only after heating for 1 day at 120 °C, the *Z* isomer being the major component.

The geometric selectivity in the reaction catalyzed by **3** favors the isomer with *trans* geometry of the double bond (*E/Z* = 6), being the same in the early stages of the reaction, which indicates that the isomers neither interconvert nor become involved in further processes. Since only the *E* isomer is detected in the first spectra, it appears that the σ -bond metathesis process occurs preferentially with a change of configuration with respect to complex **3**. The catalytic activity of the solution endures after complete transformation of complex **3**, implying that the complex has changed into the catalytic species and it is not the resting state of the catalyst. Since **3** is consumed during the dimerization

reaction, the σ -metathesis step is not rate determining in the catalytic process. Figure 4 shows no evidence of an induction period, suggesting that the formation of the catalytic species is rapid, of lower energy, with respect to the rate of formation of the enyne products.

Inspection of the ^1H NMR spectra reveals the disappearance of the indenyl protons of **3** but gives no clean spectral evidence of the organometallic products, while more information is obtained by ^{31}P NMR. After 14 h of reaction, when the solution is still active, the spectrum shows the resonance of complex **3** (δ 19.74 ppm), in addition to that of the alkynyl complex $[\text{Ru}(\eta^5\text{-C}_9\text{H}_7)(\text{dppm})(\text{C}\equiv\text{CPh})]$ (19.49 ppm), as well as two doublets at δ 62.6 and 40.9 ($J_{\text{P-P}} = 135 \text{ Hz}$) and smaller doublets at 104.7 and -24.2 ($J_{\text{P-P}} = 41 \text{ Hz}$) ppm, due to the presence of uncharacterized species bearing nonequivalent phosphorus atoms. Especially the latter peaks are typical of dppm ruthenium complexes where the bisphosphine is monodentate,²⁰ which may leave an open coordination site on the metal for catalytic activity.

Conversely, the η^3 -enyne complexes $[(\text{PP}_3)\text{Ru}\{(E)\text{-}\eta^3\text{-C}(\text{C}\equiv\text{CR})\text{=CHR}\}]\text{BF}_4$ ($\text{R} = \text{SiMe}_3, \text{Ph}$) were the only organometallic species observable in the course of the catalytic dimerization of $\text{RC}\equiv\text{CH}$ by $[\text{Ru}(\sigma\text{-C}\equiv\text{CR})(\text{PP}_3)]$.^{1f}

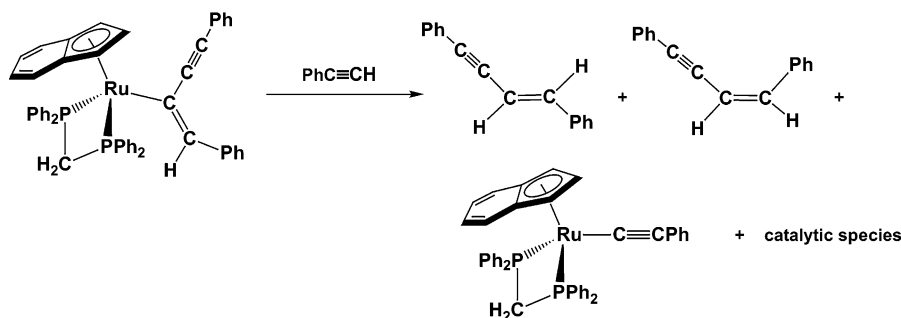
The disappearance of **3** follows clean first-order behavior. A plot of $\ln[\mathbf{3}]$ vs time is linear and yields a value of $k_{\text{obs}} = 7.7 \times 10^{-5} \text{ s}^{-1}$ for $[\text{PhC}\equiv\text{CH}] = 4.2 \text{ M}$. The rate is dependent on the concentration of $\text{PhC}\equiv\text{CH}$ (2.6 M, $k_{\text{obs}} = 3.5 \times 10^{-5} \text{ s}^{-1}$), indicating that the transformation of the σ -enyne complex is induced by the alkyne, and it is not due to complex decomposition. The transformation of complex **3** can therefore be represented as in Scheme 4.

The catalytic reaction also proceeds at lower concentration of both alkyne (2.58 M) and complex **3** (0.039 M, 1.5%), with 31% conversion of phenylacetylene after 40 h of reaction. On the other hand, in the presence of $[\text{Ru}(\text{C}\equiv\text{CPh})(\eta^5\text{-C}_9\text{H}_7)(\text{dppm})]$ (0.042 M, 1.6%) under similar experimental conditions ($[\text{PhC}\equiv\text{CH}] = 2.64 \text{ M}$, 77 °C), the formation of [(*E*)-1,4-diphenylbut-1-en-3-yne] does not exceed 3 mol per mole of the alkynyl complex.

In conclusion, the σ -enyne complex involves a lower energy pathway as well as additional formation of the active species, resulting in a better catalyst precursor than the alkynyl, the hydride, or the styryl derivatives $[\text{RuX}(\eta^5\text{-C}_9\text{H}_7)(\text{dppm})]$ ($\text{X} = \text{H}, \text{C}\equiv\text{CPh}, (E)\text{-CH=CHPh}$), which exhibit consistent catalytic activity only at high temperatures.

(20) (a) Gamasa, M. P.; Gimeno, J.; Lastra, E.; Lanfranchi, M.; Tiripicchio, A. *J. Organomet. Chem.* **1992**, *430*, C39. (b) Gamasa, M. P.; Gimeno, J.; Lastra, E.; Lanfranchi, M.; Tiripicchio, A. *J. Organomet. Chem.* **1991**, *405*, 333.

Scheme 4



Experimental Section

General Data. The reactions were carried out under dry nitrogen using standard Schlenk techniques. Solvents were dried by standard methods and distilled under nitrogen before use. The complex $[\text{RuH}(\eta^5\text{-C}_9\text{H}_7)(\kappa^2\text{-P-dppm})]$ was prepared by published methods.⁸ Infrared spectra were recorded on a Perkin-Elmer FT-1720-Y spectrometer. Mass spectra (FAB) were recorded using a VG-Autospec spectrometer, operating in the positive mode; 3-nitrobenzyl alcohol (NBA) was used as the matrix. The conductivities were measured at room temperature, in ca. 10^{-3} mol·dm⁻³ acetone solutions, with a Jenway PCM3 conductimeter. NMR spectra were recorded on a Bruker DPX-300 or AC-300 instrument operating at 300 MHz (¹H), 121.5 MHz (³¹P), and 75.4 MHz (¹³C) or a Bruker AC-200 instrument operating at 200 MHz (¹H), 81.01 MHz (³¹P), and 50.32 MHz (¹³C), using SiMe₄ or 85% H₃PO₄ as standard. Inconsistent C, H elemental analyses were found for complexes **3** and **4** due to incomplete combustion.

Synthesis of the Enynyl Complex $[\text{Ru}\{\text{(E)-}\eta^1\text{-C}(\text{C}\equiv\text{CPh})=\text{CHPh}\}(\eta^5\text{-C}_9\text{H}_7)(\kappa^2\text{-P-dppm})]$ (3**).** A solution of the hydride complex **1** (0.25 g, 0.39 mmol) and a large excess of diphenylbutadiyne (0.789 g, 3.9 mmol) in toluene (40 mL) was heated under reflux for 90 min. The solvent was then evaporated to dryness, and the brown solid residue was repeatedly washed with pentane (4 × 15 mL), to eliminate the excess of diyne, and dried under vacuum, yielding **3** as a yellow-orange solid (0.181 g, 58%). The yield of **3** was improved by proceeding as follows: the solid residue was dissolved in 50 mL of diethyl ether, cooled at -40 °C, and treated dropwise with an ethereal solution of HBF₄ (0.40 mmol). Immediately, the cationic complex **4** precipitated as a red solid. The solution was decanted and the solid washed with diethyl ether (3 × 20 mL) to eliminate the excess diyne. A solution of **4** in THF (10 mL) was treated with an equimolar amount of KO^tBu, the mixture stirred for 30 min, and the solvent removed to dryness. The residue obtained was extracted with diethyl ether and filtered to give the enynyl complex **3** in 81% yield. ³¹P{¹H} NMR (CDCl₃): δ 19.68 s. ¹H NMR (CDCl₃): δ 4.30 (dt, *J*_{HH} = 14.0 Hz, ²*J*_{HP} = 11.1 Hz, 1H, PCH_aH_bP), 4.70 (dt, *J*_{HH} = 14.0 Hz, ²*J*_{HP} = 9.8 Hz, 1H, PCH_aH_bP), 5.03 (d, *J*_{HH} = 2.6 Hz, 2H, H-1,3), 5.47 (t, *J*_{HH} = 2.6 Hz, 1H, H-2), 5.56 (s, 1H, =CH), 6.78–7.54 (m, 34H, PPh₂, =CPh, =CPh, H-4,5,6,7). ¹³C{¹H} NMR (CDCl₃): δ 47.83 (t, *J*_{CP} = 21.0 Hz, PCH₂P), 70.28 (s, C-1,3), 91.57 (s, C-2), 99.91 (s, C≡CPh), 102.32 (s, C≡CPh), 108.86 (s, C-3a,7a), 122.70 and 123.58 (s, C-4,5 and C-6,7), 123.88–132.44 (m, PPh₂, =CPh, =CPh), 134.35 (t, ²*J*_{CP} = 13.7 Hz, Ru-C), 135.46 (t, *J*_{CP} = 21.3 Hz, PC_{ipso}), 139.20 (t, *J*_{CP} = 20.4 Hz, PC_{ipso}), 145.01 (t, ³*J*_{CP} = 5.8 Hz, =CHPh). Δδ (C-3a,7a) = -21.84. IR (KBr, cm⁻¹): ν (C≡C) 2154 w. MS (FAB, *m/e*): 804 (M), 689 (M - C₉H₇), 601 (M - C₁₆H₁₁), 485 (M - C₉H₇ - C₁₆H₁₁) (correct isotope patterns observed for each fragment).

Synthesis of the Alkynylalkylidene Complex $[\text{Ru}\{\text{C}(\text{C}\equiv\text{CPh})\text{CH}_2\text{Ph}\}(\eta^5\text{-C}_9\text{H}_7)(\kappa^2\text{-P-dppm})][\text{BF}_4]$ (4**).** A stirred solution of the enynyl complex **3** (0.1 g, 0.12 mmol) in 20 mL

of diethyl ether, cooled at -40 °C, was treated dropwise with a dilute solution of HBF₄ in diethyl ether (0.13 mmol). Immediately, a red solid precipitated. The solution was decanted and the solid washed with diethyl ether (3 × 20 mL) and vacuum-dried. Yield: 94%. ³¹P{¹H} NMR (CD₂Cl₂): δ 16.09 s. ¹H NMR [CO(CD₃)₂]: δ 2.85 (s, 2H, CH₂Ph), 4.87 (bs, 1H, H-2), 5.65 (dt, *J*_{HH} = 16.0 Hz, ²*J*_{HP} = 12.8 Hz, 1H, PCH_aH_bP), 6.23 (d, *J*_{HH} = 2.6 Hz, 2H, H-1,3), 6.27 (m, 1H, PCH_aH_bP), 6.41 and 6.98 (m, 2H each, H-4,5 and H-6,7), 7.09–7.96 (m, 30H, PPh₂, CH₂Ph, =CPh). ¹³C{¹H} NMR (CD₂Cl₂): δ 47.82 (t, *J*_{CP} = 26.3 Hz, PCH₂P), 63.75 (s, CH₂Ph), 86.13 (s, C-1,3), 93.55 (s, C-2), 108.78 (t, ³*J*_{CP} = 3.1 Hz, C≡CPh), 114.85 (s, C-3a,7a), 122.60 (s, C≡CPh), 124.32 (s, C-4,5 or C-6,7), 127.01–134.42 (m, PPh₂, CH₂Ph, =CPh, C-4,5 or C-6,7), 134.76 (t, *J*_{CP} = 24.6 Hz, PC_{ipso}), 138.39 and 143.11 (s, C_{ipso}), 293.78 (t, ²*J*_{CP} = 6.4 Hz, Ru=C). Δδ (C-3a,7a) = -15.85. IR (KBr, cm⁻¹): ν (C≡C) 2132 w; (BF₄⁻) 1062 b. Conductivity (acetone, 20 °C): 108 Ω⁻¹ cm² mol⁻¹. MS (FAB, *m/e*): 805 (M⁺), 689 (M⁺ - C₉H₇ - 1), 601 (M⁺ - C₁₆H₁₂), 485 (M⁺ - C₉H₇ - C₁₆H₁₂ - 1), 421 (M⁺ - dppm) (correct isotope patterns observed for each fragment).

Rate Measurements. The ruthenium complex **1** or **3** and [(PhC≡C)₂] or PhC≡CH were dissolved in benzene-*d*₆ into an NMR tube, under argon. ¹H or ³¹P NMR spectra were collected immediately after mixing, using a macro sequence. The temperature in the NMR probe was determined from the chemical shift difference between OH and CH₂ signals of a solution of ethylene glycol containing 20% DMSO-*d*₆. The first-order rate constants were obtained from nonlinear least-squares regression analysis by fitting the exponential dependence of concentration, *c*, calculated via peak intensities (³¹P) or integration with mesitylene as internal standard (¹H), against time. The procedure yields values of *c*_∞, *k*_{obs}, and correlation coefficient (*R*). The *k*_{obs} values were checked against those obtained from straight line plots of ln *c* vs time.

X-ray Crystal Structure Determination of **3 and **4**.** X-ray-suitable single crystals were obtained by slow diffusion of pentane into toluene or of diethyl ether into dichloromethane solutions of **3** or **4**, respectively. Diffraction data were recorded on a Nonius CAD4 single-crystal diffractometer. The intensities were measured using the ω-2θ scan technique. Three standard reflections were monitored every 60 min. On all reflections, profile analysis was performed.²¹ Some double-measured reflections were averaged, and Lorentz and polarization corrections were applied. The structure was solved by Patterson interpretation and phase expansion using DIRDIF.²² Isotropic least-squares refinement on *F*² was done using

(21) (a) Lehman, M. S.; Larsen, F. K. *Acta Crystallogr. A* **1974**, *30*, 580. (b) Grant, D. F.; Gabe, E. J. *J. Appl. Crystallogr.* **1978**, *11*, 114.

(22) Beurskens, P. T.; Admiraal, G.; Beurskens, G.; Bosman, W. P.; Garcia-Granda, S.; Gould, R. O.; Smits, J. M. M.; Smykalla, C. *The DIRDIF Program System; Technical Report of the Crystallographic Laboratory*; University of Nijmegen: Nijmegen, The Netherlands, 1996.

SHELXL97.²³ Absorption correction was applied to **3** by means of XABS2.²⁴ During the final stages of the refinements, all positional parameters and the anisotropic temperature factors of all the non-H atoms were refined. The H atoms were geometrically located and refined riding with common isotropic thermal parameters. Atomic scattering factors were taken from *International Tables for X-ray Crystallography*.²⁵ Plots were made with the EUCLID package.²⁶ Geometrical calculations were made with PARST.²⁷ All calculations were made at the

(23) Sheldrick, G. M. *SHELXL-97, Program for the Refinement of Crystal Structures*; University of Göttingen, 1997.

(24) Parkin, S.; Moezzi, B.; Hope, H. *J. Appl. Crystallogr.* **1995**, *28*, 53.

(25) *International Tables for X-ray Crystallography*; Kynoch Press: Birmingham (Present distributor: Kluwer Academic Publishers: Dordrecht), 1974; Vol. IV.

(26) Spek, A. L. *PLATON, a multipurpose crystallographic tool*; Utrecht University: Utrecht, The Netherlands, 2000.

(27) Nardelli, M. *Comput. Chem.* **1983**, *7*, 95.

Scientific Computer Centre of the University of Oviedo. The most relevant crystal and refinement data are collected in Table 3.

Acknowledgment. We thank COST CHEMISTRY Action D12 (WG D12/0025/99), Ministerio de Ciencia y Tecnología of Spain (MCT-00-BQU-0227), CICYT (BQU2000-0219), and FICYT (PR-01-GE-4) for financial support.

Supporting Information Available: NMR spectra of complexes **3** and **4**, kinetic plots, X-ray crystallographic data of **3** and **4**, including tables of atomic coordinates, thermal parameters, bond distances, and bond angles. This material is available free of charge via the Internet at <http://pubs.acs.org>.

OM020483A